

A parameterized equation of state for dark energy and Hubble Tension

Jing-Ya Zhao,¹ Tong-Yu He,¹ Jia-Jun Yin,¹ Zhan-Wen Han,^{1,2} and Rong-Jia Yang^{a1,3,4,5,†}

¹*College of Physics Science and Technology,*

Hebei University, Baoding 071002, China

²*Yunnan Observatories, Chinese Academy of Sciences, Kunming 650216, China*

³*Hebei Key Lab of Optic-Electronic Information and Materials,*

Hebei University, Baoding 071002, China

⁴*National-Local Joint Engineering Laboratory of New Energy Photoelectric Devices,*

Hebei University, Baoding 071002, China

⁵*Key Laboratory of High-prcision Computation and*

Application of Quantum Field Theory of Hebei Province,

Hebei University, Baoding 071002, China

Abstract

We propose a parameterized equation of state for dark energy and perform observational tests with the Hubble parameter measurements, the Pantheon supernova sample, baryon acoustic oscillations, and DESI DR2 data. We obtain the best-fit values for the parameters as: $H_0 = 73.96 \pm 0.16$, $\Omega_m = 0.2434 \pm 0.0079$, and $\alpha = -0.00049 \pm 0.00092$, demonstrating that the model exhibits a high degree of consistency with astronomical observations and provides a promising parameterized method for addressing the Hubble tension.

Keywords: Equation of state, Hubble tension, dark energy

^a Corresponding author

[†] yangrongjia@tsinghua.org.cn

I. INTRODUCTION

One of the most important discoveries in modern cosmology is that the Universe is currently undergoing an accelerated expansion, which poses a challenge to general relativity as a complete theory of gravity. Under the assumption that general relativity remains valid on cosmological scales, this phenomenon requires the introduction of an unknown energy component, commonly referred to as dark energy. The Λ CDM framework continues to be the leading and most widely supported description of dark energy. However, it suffers from several long-standing theoretical difficulties, including the cosmological constant problem [1], characterized by the enormous discrepancy between theoretical expectations and observational measurements; the coincidence problem [2], which asks why the energy densities of dark energy and matter are of the same order of magnitude at the present epoch; and the so-called age problem discussed in certain observational contexts [3]. Moreover, a pronounced discrepancy persists between determinations of the Hubble constant derived from early- and late-universe observations.

In the contemporary cosmological framework, the Hubble constant H_0 , which characterizes the present expansion rate of the Universe, plays a central role in probing the fundamental properties of both dark energy and dark matter. Current determinations of H_0 rely mainly on two independent approaches: indirect constraints from early Universe probes [4] and direct measurements from late Universe observations [5]. Early Universe measurements infer the value of the Hubble constant through precision observations of cosmic microwave background (CMB) anisotropies within the Λ CDM framework. Based on the final Planck data release, the most precise early Universe determination yields $H_0 = 67.4 \pm 0.5 \text{ km s}^{-1} \text{ Mpc}^{-1}$ [6]. In contrast, late time measurements based on the combined Cepheid and supernova samples give a significantly higher value, $H_0 = 73.04 \pm 1.04 \text{ km s}^{-1} \text{ Mpc}^{-1}$ [7]. The discrepancy between these two determinations reaches the level of approximately 5σ , well beyond the range expected from statistical uncertainties. This tension is now widely known as the Hubble tension [8–12]. Related aspects of this problem have been investigated in Refs. [13–16]. In addition to the discrepancy between early and late Universe measurements, indications of tension have also been reported in certain low-redshift observational data. Despite extensive efforts, including modifications of early Universe physics [17], the introduction of new physical components [18], and detailed reassessments of potential sys-

tematic effects, the Hubble tension persists as one of the most striking challenges in modern cosmology.

Since the Hubble tension is primarily established within the Λ CDM framework, it may signal the need for dynamical dark energy beyond a simple cosmological constant. Analysis of observational Hubble data or Dark Energy Spectroscopic Instrument (DESI) DR2 data with a model-independent method implies a dynamical dark energy [19–21]. Recent observations from the DESI data, combined with independent measurements of the Hubble parameter, also indicates a statistical preference for dynamical dark energy models over the standard Λ CDM scenario [22–25].

These developments provide strong motivation to investigate concrete realizations of dynamical dark energy. Here we propose a parameterized equation of state (EoS) for dark energy and constrain the parameters with observational data from Hubble parameter measurements, the Pantheon supernova sample, baryon acoustic oscillations (BAO), and DESI DR2 data. The value of H_0 we obtain is consistent with that obtained from the combined Cepheid and supernova samples [7], which can alleviate the Hubble tension.

The structure of this paper is as follows. Section II provides a concise overview of the k-essence cosmology considered in this work. In Section III, we employ Markov Chain Monte Carlo (MCMC) techniques to constrain the model parameters using current observational datasets. Section IV presents a discussion of the resulting constraints, and Section V summarizes our main conclusions.

II. THE PARAMETERIZED EQUATION OF STATE

There are generally two parameterization methods for dark energy cosmology: one is to parameterize the Hubble function, and the other is to parameterize the EoS of dark energy. Inspired by [26], we suggest the parameterized EoS for dark energy takes the form as follows

$$w = -\frac{1}{1 + \alpha(1 + z)^6}, \quad (1)$$

where α is a positive constant in [26], here we relax this restriction and treat α as a general constant, so when $\alpha = 0$, the model reduces to Λ CDM; if $\alpha < 0$, the model behaves like phantom dark energy; if $\alpha > 0$, the model evolves like quintessence. With Eq. (1), the

Friedmann equation in a flat Friedmann-Robertson-Walker-Lemaître takes the form of

$$H^2(z) = H_0^2 [\Omega_m(1+z)^3 + (1-\Omega_m)f(z)], \quad (2)$$

where Ω_m is the present value of dimensionless energy density for dark and baryonic matter, and

$$f(z) = \sqrt{\frac{1+\alpha(1+z)^6}{1+\alpha}}. \quad (3)$$

In the model we consider, H_0 , Ω_m , and α are the parameters needed to be constrained with observational data, which is exactly the main content of the next section.

III. METHODOLOGY AND DATA

Building on the parameterized EoS for dark energy developed earlier, we next evaluate whether the approximate parameter values are capable of reproducing the observational data relevant to today's Universe. For this purpose, we primarily utilize four distinct datasets: the Hubble parameter dataset comprising 62 data points, the Pantheon sample of 1701 supernovae, a compilation of six BAO measurements, and a set of eight F parameter data points derived from BAO observations.

Before proceeding with the joint constraint of the model using the datasets, it is necessary to introduce the MCMC [27]: which operates on the core principle of constructing a specialized Markov chain based on the model. When the number of iterations becomes large enough, the resulting sample set converges toward the posterior distribution of the model parameters. A notable feature of this method is that the convergence outcome is independent of the initial values.

The specific computational procedure is described as follows: First, we explicitly specify the parameters to be constrained (H_0 , Ω_m , and α) based on the cosmological model proposed in the preceding section, assigning physically motivated priors to each parameter and constructing the corresponding likelihood function. During the sampling process, we combine the four distinct data sets employing a joint likelihood function, which appropriately weights and combines the error distributions across the different observational datasets.

In this process, we utilize the emcee package [28] and present the results in the form of two-dimensional contour plots with confidence intervals of 68.3% (1σ) and 95.5% (2σ).

A. Observational Hubble data

One of the most critical data sets for constraining cosmological models is the observational Hubble data (OHD), which is obtained through direct measurements of the expansion rate. In this study, we employ the differential age method to determine the Hubble parameter as a function of redshift [29, 30],

$$H(z) = -\frac{1}{1+z} \frac{dz}{dt}. \quad (4)$$

The OHD obtained through direct measurements of the cosmic expansion rate represents one of the most critical datasets for constraining cosmological models [31–33]. The redshift dependence of the Hubble parameter is determined using the differential age method. Also known as the cosmic chronometer approach, this technique computes the expansion rate at a given cosmic epoch by measuring the age difference (dt) between passively evolving galaxies formed at different redshifts, in conjunction with the corresponding redshift interval (dz). As shown in Eq. 4, this enables a direct determination of the Hubble parameter without relying on assumptions from any specific cosmological model.

The cosmic chronometer approach provides 34 $H(z)$ measurements derived from the cosmic expansion rate [34–37], while an additional 28 $H(z)$ measurements are obtained from the analysis of BAO peaks in the galaxy power spectrum [38–46], as collected in [19]. The cosmic chronometer method offers the distinctive advantage of being model-independent, whereas the BAO technique extends observational coverage over a broader redshift range. Owing to its model-independent nature, the cosmic chronometer method serves as a key diagnostic for probing dark energy models and addressing outstanding challenges such as the Hubble tension, thereby holding particular value in contemporary cosmological research.

The dataset spans redshifts from $z = 0$ up to $z = 1.965$. For consistency, we adopt a representative value of $H_0 = 70 \text{ km s}^{-1} \text{ Mpc}^{-1}$ throughout the analysis [47]. Subsequently, we performed a maximum likelihood analysis to determine the mean values of the model parameters (H_0 , Ω_m and α). The χ^2 function [48] used for OHD data is given by

$$\chi_H^2 = \sum_{i=1}^{62} \frac{[H_i^{\text{th}}(H_0, \Omega_m, \alpha) - H_i^{\text{obs}}(z_i)]^2}{\sigma_H^2(z_i)}, \quad (5)$$

The symbol H_i^{th} represents the theoretically computed Hubble parameter, while H_i^{obs} indicates its observed counterpart. The factor σ_H^2 stands for the observational error variance of

$H(z)$ at the redshift z_i . As shown in Figure 1, we derived the best fit values of the model parameters (H_0 , α and Ω_m) following the contours of the confidence levels of 68% (1σ) and 95% (2σ).

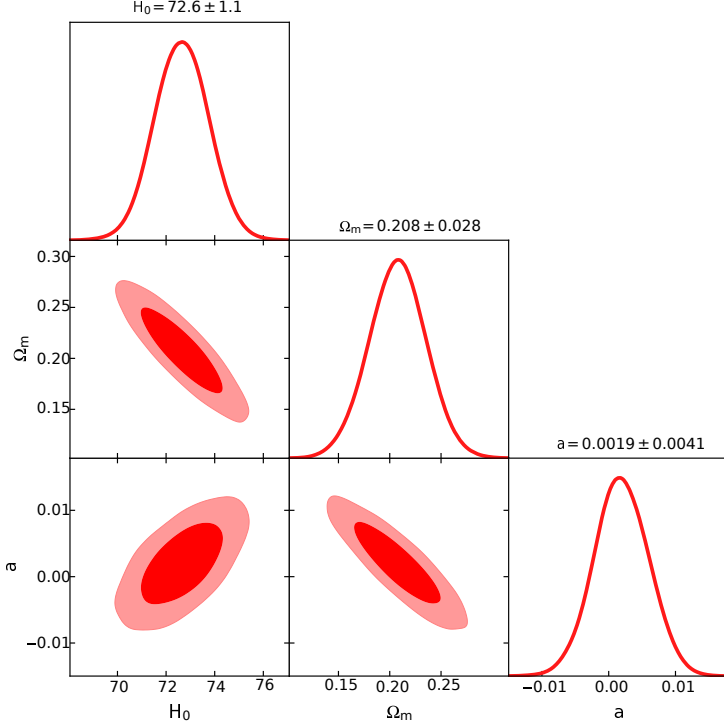


FIG. 1. The inferred best-fit model parameters along with their 1σ and 2σ confidence regions based on the Hubble datasets.

At 1σ confidence level, the best-fit values are: $H_0 = 72.6 \pm 1.1 \text{ km s}^{-1} \text{ Mpc}^{-1}$, $\Omega_m = 0.208 \pm 0.028$ and $\alpha = 0.0019 \pm 0.0041$. Furthermore, Figure 2 presents the Hubble data error bar plot, compared to the Λ CDM model with $H_0 = 67.4 \text{ km s}^{-1} \text{ Mpc}^{-1}$ and $\Omega_m = 0.315$ [6]. This result demonstrates that our framework can accurately describe the Hubble observational data set.

B. Pantheon+ data

SNeIa are thermonuclear explosions that occur when a white dwarf accretes sufficient mass to exceed the Chandrasekhar limit. Owing to their remarkably uniform luminosity characteristics, SNeIa serve as excellent standard candles for investigating cosmic dynamics. Although only a few dozen SNeIa light curves had been recorded by 1980s, subsequent obser-

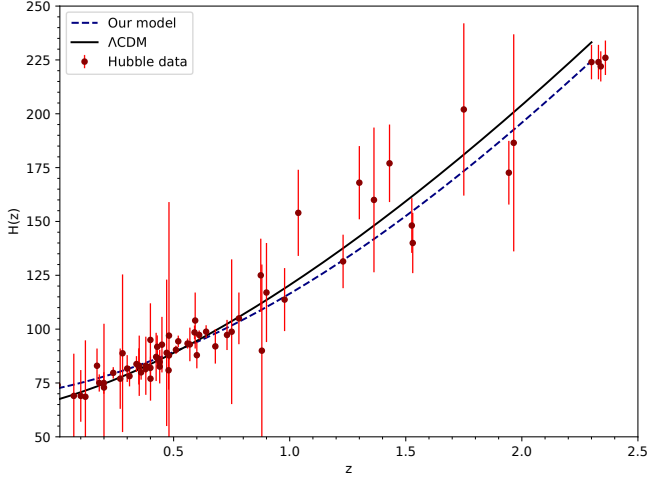


FIG. 2. The reconstructed Hubble function $H(z)$ as a function of redshift inferred from observational Hubble data. The dotted lines shows the prediction of our model, while the solid black curve denotes the Λ CDM scenario.

vational advances have ushered in the modern high-precision era of cosmology. In this study, we used the most comprehensive supernova sample to date—the Pantheon+ dataset—which incorporates observations from several major international surveys including Pan-STARRS1 (PS1), the Dark Energy Survey (DES), the Supernova Legacy Survey (SNLS), and the Sloan Digital Sky Survey (SDSS) [7]. The complete sample comprises 1,701 SNeIa spectroscopically confirmed subsets spanning a wide redshift range, including low redshift, intermediate redshift, and high redshift subsets [49]. Our methodology involves comparing theoretical distance moduli with observed values to constrain cosmological parameters, where the distance modulus for each supernova is calculated using the standard relation

$$\mu_{\text{th}}(z) = 5 \log_{10} [d_{\text{L}}(z)/\text{Mpc} + 25], \quad (6)$$

where the luminosity distance $d_{\text{L}}(z)$ is given by

$$d_{\text{L}}(z) = (1 + z) \int_0^z \frac{dz'}{H(z')} \quad (7)$$

The chi-square function χ^2 for Pantheon+ data is

$$\chi_{\text{SN}}^2 = \sum_{i,j=1}^{1701} \Delta \mu_i (C_{\text{SN}}^{-1})_{ij} \Delta \mu_j \quad (8)$$

Here, C_{SN} is the covariance matrix provided in [50]. In addition, $\Delta\mu_i$ denotes the difference between the observationally inferred distance modulus and the theoretical prediction computed from the model parameters. Unlike the previous approach, we now adopt $\chi^2_{\text{H}} + \chi^2_{\text{SN}}$ as

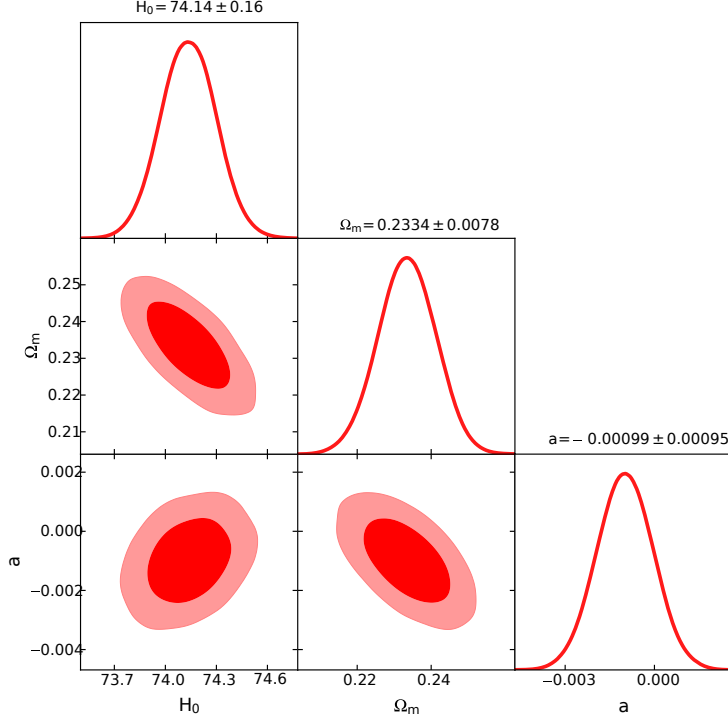


FIG. 3. Best-fit parameter estimates together with their 1σ and 2σ confidence regions derived from the combined Hubble and Pantheon+ observational samples.

the minimization constraint for the model parameters H_0 , Ω_m , and α . Here, we utilize both the Hubble dataset and Pantheon+ dataset to obtain the best-fit values. As shown in Figure 3, the results are presented with the confidence level contours 1σ and 2σ . At 1σ confidence level, the best-fit values are: $H_0 = 74.14 \pm 0.16 \text{ km s}^{-1} \text{ Mpc}^{-1}$, $\Omega_m = 0.2334 \pm 0.0078$ and $\alpha = -0.00099 \pm 0.00095$. Additionally, we present the error bar plot of the supernova data in Figure 4, where we compare our model with the Λ CDM model. Our model demonstrates excellent consistency with the combined Hubble+Pantheon+ dataset.

C. BAO data

The physical origin of BAO can be traced back to thermodynamic processes in the early Universe. BAO not only serves as a “standard ruler” for measuring the cosmic expansion

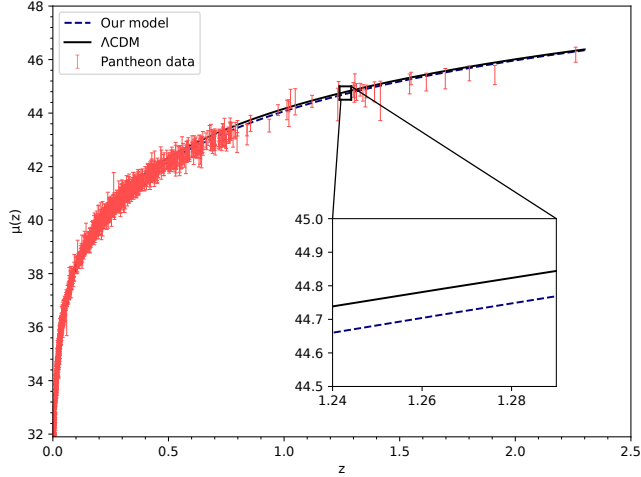


FIG. 4. The predicted distance modulus μ_z as a function of redshift z for both our model and the Λ CDM model, using parameter constraints obtained from the combined Hubble and Pantheon+ data.

z_{BAO}	0.106	0.2	0.35	0.44	0.6	0.73
$\frac{d_A(z_*)}{D_V(z_{\text{BAO}})}$	30.95 ± 1.46	17.55 ± 0.60	10.11 ± 0.37	8.44 ± 0.67	6.69 ± 0.33	5.45 ± 0.31

TABLE I. Values of $d_A(z_*)/D_V(z_{\text{BAO}})$ for distinct values of z_{BAO} .

history but also plays a crucial role in constraining the EoS of dark energy. In constraining cosmological model parameters, BAO achieves precise limitations on cosmic models by combining measurements of the sound horizon scale (r_s) imprinted in galaxy clustering patterns with redshift evolution information [51]. Here, we utilize a composite data set comprising six distinct BAO measurements across different redshift ranges. The BAO signatures within the matter power spectrum yield measurements of the Hubble parameter $H(z)$ and the angular diameter distance $d_A(z)$. They may be written as

$$d_A(z) = \int_0^z \frac{dz'}{H(z')}. \quad (9)$$

The parameter $D_V(z)$, constructed from the angular diameter distance and the Hubble expansion rate, is expressed as [52]

$$D_V(z) = \left[d_A^2(z) \frac{z}{H(z)} \right]^{1/3} \quad (10)$$

The chi-square function χ_{BAO}^2 for the BAO data is given by the following expression

$$\chi_{\text{BAO}}^2 = \mathbf{X}^T \mathbf{C}_{\text{BAO}}^{-1} \mathbf{X}, \quad (11)$$

where

$$\mathbf{X} = \begin{pmatrix} \frac{d_A(z_*)}{D_V(0.106)} - 30.95 \\ \frac{d_A(z_*)}{D_V(0.2)} - 17.55 \\ \frac{d_A(z_*)}{D_V(0.35)} - 10.11 \\ \frac{d_A(z_*)}{D_V(0.44)} - 8.44 \\ \frac{d_A(z_*)}{D_V(0.6)} - 6.69 \\ \frac{d_A(z_*)}{D_V(0.73)} - 5.45 \end{pmatrix} \quad (12)$$

The inverse covariance matrix C_{BAO}^{-1} is referenced in [53], with the six BAO data sets presented in Table I. Photon decoupling occurred at redshift $z = 1091$, precisely determined through detailed observations and spectral analysis of the CMB, ultimately producing the CMB radiation we observe today [54].

We constrain the cosmological parameters H_0 , Ω_m , and α by minimizing the combined chi-square statistic $\chi_H^2 + \chi_{\text{SN}}^2 + \chi_{\text{BAO}}^2$, utilizing joint datasets from Hubble Space Telescope observations, the Pantheon+ supernova sample, and BAO measurements. The best-fit values are shown in Figure 5, with constraints of the 1σ confidence level resulting in $H_0 = 74.15 \pm 0.17 \text{ km s}^{-1} \text{ Mpc}^{-1}$, $\Omega_m = 0.2327 \pm 0.0084$, and $\alpha = -0.0013 \pm 0.0011$.

D. DESI DR2 data

The most precise BAO measurements to date have been provided by DESI, which has observed millions of galaxies and quasars. This unprecedented data set enables the reconstruction of high-fidelity 3D maps of the cosmic web, thereby yielding precise determinations of the expansion history of the Universe and imposing stringent constraints on the EoS of dark energy.

The key data set for our analysis are the F data from the DESI DR2 [55] (see Table I). In DESI, these measurements are expressed in terms of dimensionless ratios D_M/r_d , D_V/r_d , and D_H/r_d , representing the transverse comoving, angle-averaged, and Hubble distances, respectively, all scaled by the comoving sound horizon r_d at the drag epoch. The function

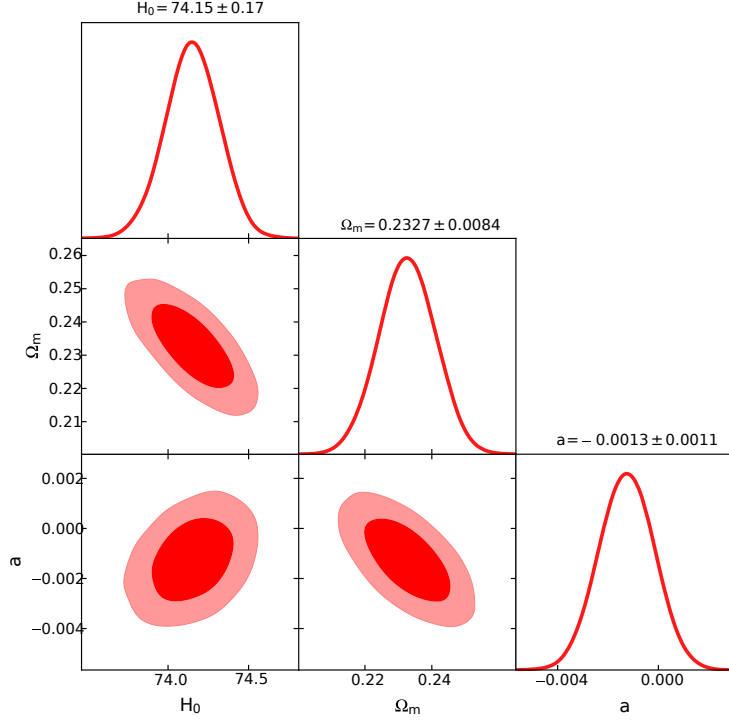


FIG. 5. The inferred best-fit model parameters, along with the corresponding 1σ and 2σ confidence contours, as constrained by the combined Hubble, Pantheon+, and BAO observational samples.

F is defined as $F \equiv D_{\text{M}}/D_{\text{H}}$. For a spatially flat Universe, the F function takes the form

$$F = E(z) \int_0^z \frac{1}{E(z')} dz', \quad (13)$$

where $E(z) = H(z)/H_0$. The chi-square function χ_{F}^2 for the F data takes the following form

$$\chi_{\text{F}}^2 = \sum_{i=1}^8 \frac{[F_i^{\text{th}}(H_0, \Omega_{\text{m}}, \alpha) - F_i^{\text{obs}}(z_i)]^2}{\sigma_{\text{F}}^2(z_i)},$$

where F_i^{th} denotes the theoretical value of the function F , while F_i^{obs} represents the observed data, with σ_{F}^2 characterizing the standard error of the observed measurement $F(z)$ at the redshift z_i . As illustrated in Figure 6, we have determined the best-fit values for the model parameters H_0 , Ω_{m} , and α following the contours 1σ and 2σ . At the 1σ confidence level, the constrained parameters yield: $H_0 = 73.96 \pm 0.16 \text{ km s}^{-1} \text{ Mpc}^{-1}$, $\Omega_{\text{m}} = 0.2434 \pm 0.0079$ and $\alpha = -0.00049 \pm 0.00092$. These results are presented in a comprehensive way in Figure 6, which displays both the parameter constraints and their correlation properties.

index	z	F
z_1	0.510	0.622 ± 0.017
z_2	0.706	0.892 ± 0.021
z_3	0.922	1.232 ± 0.021
z_4	0.934	1.223 ± 0.019
z_5	0.955	1.220 ± 0.033
z_6	1.321	1.948 ± 0.045
z_7	1.484	2.386 ± 0.136
z_8	2.330	4.518 ± 0.097

TABLE II. F data obtained from *BAO* measurement.[55]

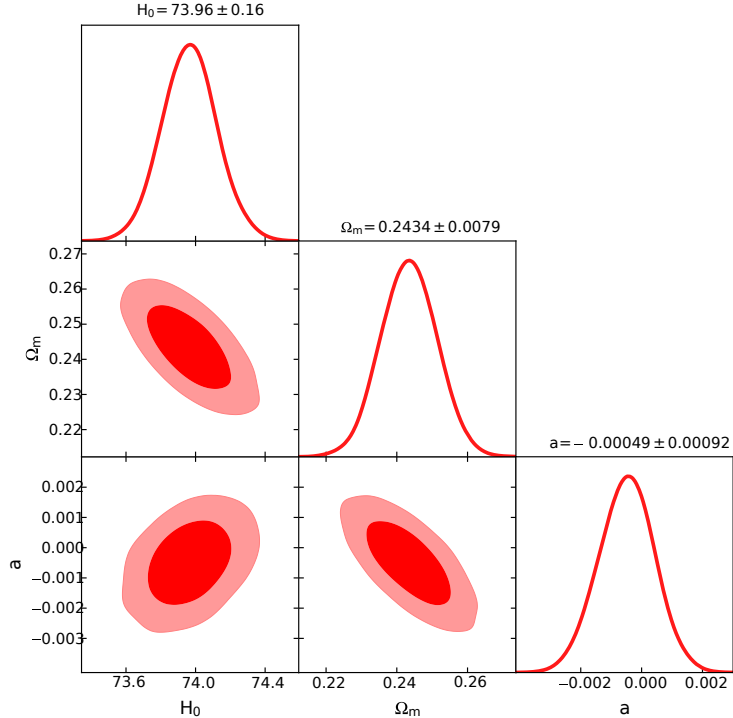


FIG. 6. Best-fit constraints on the model parameters with the corresponding 1σ and 2σ confidence contours derived from the combined Hubble, Pantheon+, BAO, and F data.

IV. RESULTS

In this section, we present a comprehensive discussion of the results obtained above. Through MCMC analysis, we have systematically constrained the model parameters (H_0 ,

Data	H_0 (km/s/Mpc)	Ω_m	α
Prior	(64.9, 76.8)		
Hubble	72.6 ± 1.1	0.208 ± 0.028	0.0019 ± 0.0041
Hubble+Pantheon	74.14 ± 0.16	0.2334 ± 0.0078	-0.00099 ± 0.00095
Hubble+Pantheon+BAO	74.15 ± 0.17	0.2327 ± 0.0084	-0.0013 ± 0.0011
Hubble+Pantheon+BAO+F	73.96 ± 0.16	0.2434 ± 0.0079	-0.00049 ± 0.00092

TABLE III. A summary of the outcomes inferred from the four datasets.

Ω_m , and α) using progressively combined datasets: (i) Hubble data alone, (ii) Hubble + Pantheon, (iii) Hubble + Pantheon + BAO, and (iv) Hubble + Pantheon + BAO + F data. Firstly, the Hubble parameter is constrained by using a Hubble data set comprising 62 data points. In Figure 1, the best-fit values of the model parameters are determined, producing a Hubble constant of $H_0 = 72.6 \pm 1.1 \text{ km s}^{-1} \text{ Mpc}^{-1}$, $\Omega_m = 0.208 \pm 0.028$ and $\alpha = 0.0019 \pm 0.0041$, implying that the dark energy behaves like quintessence. Figure 2 shows that our model is consistent with both the standard Λ CDM paradigm and the observational data. In order to mitigate the uncertainties in the model parameters, 1701 data points from the Pantheon sample are introduced. Figure 3 presents the joint constraints from the Hubble and Pantheon samples [47], giving the best-fit values: $H_0 = 74.14 \pm 0.16 \text{ km s}^{-1} \text{ Mpc}^{-1}$, $\Omega_m = 0.2334 \pm 0.0078$ and $\alpha = -0.00099 \pm 0.00095$, indicating that the dark energy behaves like phantom. A significant reduction in the uncertainty of the Hubble parameter was achieved through the joint constraints with the Pantheon compilation. Figure 4 shows that our model provides an excellent fit to the Pantheon data while being close to the standard Λ CDM paradigm. We included six BAO data points in the constraint analysis to improve precision and find: $H_0 = 74.15 \pm 0.17 \text{ km s}^{-1} \text{ Mpc}^{-1}$, $\Omega_m = 0.2327 \pm 0.0084$ and $\alpha = -0.0013 \pm 0.0011$, also meaning a phantom behavior. We then included eight F data points from DESI DR2 in the analysis and derived the fitting results: $H_0 = 73.96 \pm 0.16 \text{ km s}^{-1} \text{ Mpc}^{-1}$, $\Omega_m = 0.2434 \pm 0.0079$ and $\alpha = -0.00049 \pm 0.00092$, still suggesting a phantom dark energy. Table 3 shows that the precision of the constraints in H_0 , Ω_m and α progressively improves as more observational data are included. To validate our model, we marked its Hubble and Pantheon error bars against the standard Λ CDM model. Figures 2 and 4 demonstrate its excellent concordance with observational datasets.

Table 3 shows the variations in the best-fit parameters (H_0 , Ω_m , α) depending on the data set used. The OHD only fit diverges significantly from the results of the three joint analyzes, which are mutually consistent. This indicates that the Hubble dataset, likely due to its limited volume, can yield biased constraints when used independently. The inferred parameters demonstrate robustness against the choice of dataset. The Hubble constant H_0 is largely insensitive, while the matter density parameter Ω_m exhibits only marginal variations within the range of 0.217 to 0.2427. The value of α demonstrates higher sensitivity, as evidenced by its variation and subsequent convergence towards a precise value under tightening constraints from larger datasets. The value of the Hubble constant obtained in this work exhibits a noticeable deviation from the Planck 2018 result derived within the Λ CDM framework [6], while remaining in good agreement with the late-time measurements based on the Cepheid–supernova sample [7]. This tension highlights that the inference of H_0 is not robust across different models and is particularly sensitive to the underlying cosmological framework.

V. CONCLUSION

We have proposed a parameterized EoS for dark energy which was constrained through MCMC using a combination of Hubble, Pantheon, BAO, and DESI DR2 data.

To minimize the impact of systematic uncertainties and any potential biases inherent in the observational data, we adopted the following methodology: we performed cross-validation of the constraints using multiple independent datasets to mitigate the influence of systematic errors from any single dataset. Furthermore, in selecting the datasets for our constraints, we specifically employed those that have undergone extensive cross-calibration and systematic error correction by other researchers. In addition, we conducted a comprehensive error propagation analysis incorporating error terms into the Monte Carlo likelihood function. Despite implementing extensive measures to minimize uncertainties throughout our analysis and simulations, the complete elimination of biases and systematic errors from observational data remains challenging and ultimately unattainable.

The model was further validated against Hubble, Pantheon+, BAO, and DESI DR2 datasets, and the best-fit parameter values are constrained to $H_0 = 73.96 \pm 0.16 \text{ km s}^{-1} \text{ Mpc}^{-1}$, $\Omega_m = 0.2434 \pm 0.0079$ and $\alpha = -0.00049 \pm 0.00092$, indicating the dark energy behaves like phantom. As provided in Table II, we have reported the upper and lower bounds for each

parameter. It is clearly evident that the results demonstrate minimal sensitivity to these errors. Furthermore, the confidence intervals also show that these uncertainties are small and do not substantially influence the conclusions reached in this work.

These results show excellent agreement with Cepheid-calibrated supernova observations, but exhibit a significant discrepancy (exceeding reported uncertainties) compared to the 2018 Planck CMB measurements. This inconsistency, known as the Hubble tension, arises primarily from the elevated value of the Hubble constant H_0 obtained from late Universe probes compared to the value inferred from the standard Λ CDM model applied to early Universe data. In the model we proposed, this tension has been alleviated. If there is more data in the future, our research can be further expanded.

ACKNOWLEDGMENTS

This study is supported in part by the National Natural Science Foundation of China (Grant No. 12333008).

- [1] S. M. Carroll, The Cosmological constant, *Living Rev. Rel.* 4 (2001) 1. [arXiv:astro-ph/0004075](https://arxiv.org/abs/astro-ph/0004075), doi:10.12942/lrr-2001-1.
- [2] I. Zlatev, L.-M. Wang, P. J. Steinhardt, Quintessence, cosmic coincidence, and the cosmological constant, *Phys. Rev. Lett.* 82 (1999) 896–899. [arXiv:astro-ph/9807002](https://arxiv.org/abs/astro-ph/9807002), doi:10.1103/PhysRevLett.82.896.
- [3] R.-J. Yang, S. N. Zhang, The age problem in Λ CDM model, *Mon. Not. Roy. Astron. Soc.* 407 (2010) 1835–1841. [arXiv:0905.2683](https://arxiv.org/abs/0905.2683), doi:10.1111/j.1365-2966.2010.17020.x.
- [4] R. Durrer, A. Neronov, Cosmological Magnetic Fields: Their Generation, Evolution and Observation, *Astron. Astrophys. Rev.* 21 (2013) 62. [arXiv:1303.7121](https://arxiv.org/abs/1303.7121), doi:10.1007/s00159-013-0062-7.
- [5] S. S. da Costa, D. R. da Silva, Á. S. de Jesus, N. Pinto-Neto, F. S. Queiroz, The H_0 trouble: confronting non-thermal dark matter and phantom cosmology with the CMB, BAO, and Type Ia supernovae data, *JCAP* 04 (2024) 035. [arXiv:2311.07420](https://arxiv.org/abs/2311.07420), doi:10.1088/1475-7516/2024/04/035.

[6] N. Aghanim, et al., Planck 2018 results. VI. Cosmological parameters, *Astron. Astrophys.* 641 (2020) A6, [Erratum: *Astron. Astrophys.* 652, C4 (2021)]. [arXiv:1807.06209](https://arxiv.org/abs/1807.06209), doi:10.1051/0004-6361/201833910.

[7] A. G. Riess, et al., A Comprehensive Measurement of the Local Value of the Hubble Constant with $1 \text{ km s}^{-1} \text{ Mpc}^{-1}$ Uncertainty from the Hubble Space Telescope and the SH0ES Team, *Astrophys. J. Lett.* 934 (1) (2022) L7. [arXiv:2112.04510](https://arxiv.org/abs/2112.04510), doi:10.3847/2041-8213/ac5c5b.

[8] E. Di Valentino, et al., Snowmass2021 - Letter of interest cosmology intertwined II: The hubble constant tension, *Astropart. Phys.* 131 (2021) 102605. [arXiv:2008.11284](https://arxiv.org/abs/2008.11284), doi:10.1016/j.astropartphys.2021.102605.

[9] B. Wang, M. López-Corredoira, J.-J. Wei, The Hubble tension survey: A statistical analysis of the 2012–2022 measurements, *Mon. Not. Roy. Astron. Soc.* 527 (3) (2023) 7692–7700. [arXiv:2311.18443](https://arxiv.org/abs/2311.18443), doi:10.1093/mnras/stad3724.

[10] L. Verde, T. Treu, A. G. Riess, Tensions between the Early and the Late Universe, *Nature Astron.* 3 (2019) 891. [arXiv:1907.10625](https://arxiv.org/abs/1907.10625), doi:10.1038/s41550-019-0902-0.

[11] E. Abdalla, et al., Cosmology intertwined: A review of the particle physics, astrophysics, and cosmology associated with the cosmological tensions and anomalies, *JHEAp* 34 (2022) 49–211. [arXiv:2203.06142](https://arxiv.org/abs/2203.06142), doi:10.1016/j.jheap.2022.04.002.

[12] E. Di Valentino, et al., The CosmoVerse White Paper: Addressing observational tensions in cosmology with systematics and fundamental physics, *Phys. Dark Univ.* 49 (2025) 101965. [arXiv:2504.01669](https://arxiv.org/abs/2504.01669), doi:10.1016/j.dark.2025.101965.

[13] M. G. Dainotti, et al., A New Master Supernovae Ia sample and the investigation of the Hubble tension, *JHEAp* 48 (2025) 100405. [arXiv:2501.11772](https://arxiv.org/abs/2501.11772), doi:10.1016/j.jheap.2025.100405.

[14] T.-Y. He, J.-J. Yin, Z.-Y. Wang, Z.-W. Han, R.-J. Yang, A new parametrization of Hubble function and Hubble tension, *JCAP* 09 (2024) 028. [arXiv:2405.17212](https://arxiv.org/abs/2405.17212), doi:10.1088/1475-7516/2024/09/028.

[15] S. Paul, R. K. Das, S. Pan, Parametrizing the Hubble function instead of dark energy: Many possibilities, *Phys. Rev. D* 112 (4) (2025) 043542. [arXiv:2508.08072](https://arxiv.org/abs/2508.08072), doi:10.1103/177j-mmhw.

[16] P. A. Milne, R. J. Foley, P. J. Brown, G. Narayan, The Changing Fractions of Type ia Supernova Nuv–optical Subclasses With Redshift, *Astrophys. J.* 803 (1) (2015) 20. [arXiv:1408.1706](https://arxiv.org/abs/1408.1706), doi:10.1088/0004-637X/803/1/20.

[17] F. Niedermann, M. S. Sloth, Resolving the Hubble tension with new early dark energy, *Phys. Rev. D* 102 (6) (2020) 063527. [arXiv:2006.06686](https://arxiv.org/abs/2006.06686), doi:10.1103/PhysRevD.102.063527.

[18] A. Gogoi, R. K. Sharma, P. Chanda, S. Das, Early Mass-varying Neutrino Dark Energy: Nugget Formation and Hubble Anomaly, *Astrophys. J.* 915 (2) (2021) 132. [arXiv:2005.11889](https://arxiv.org/abs/2005.11889), doi:10.3847/1538-4357/abfe5b.

[19] R.-J. Yang, Possible evidences from $H(z)$ parameter data for physics beyond Λ CDM, *New Astron.* 108 (2024) 102180. doi:10.1016/j.newast.2023.102180.

[20] R.-J. Yang, Possible evidences for physics beyond Λ CDM from DESI DR2 data (6 2025). [arXiv:2506.15739](https://arxiv.org/abs/2506.15739).

[21] R.-J. Yang, Results from Hubble Parameter Data: Oscillating Dark Energy?, *Res. Astron. Astrophys.* 26 (1) (2026) 015003. doi:10.1088/1674-4527/ae1720.

[22] A. G. Adame, et al., DESI 2024 VI: cosmological constraints from the measurements of baryon acoustic oscillations, *JCAP* 02 (2025) 021. [arXiv:2404.03002](https://arxiv.org/abs/2404.03002), doi:10.1088/1475-7516/2025/02/021.

[23] G. N. Gadbail, S. Mandal, P. K. Sahoo, K. Bamba, Reconstruction of the scalar field potential in nonmetricity gravity through Gaussian processes, *Phys. Lett. B* 860 (2025) 139232. [arXiv:2411.00051](https://arxiv.org/abs/2411.00051), doi:10.1016/j.physletb.2024.139232.

[24] A. Samaddar, S. S. Singh, CPL-parametrized cosmic expansion in Galileon gravity: Constraints from recent data, *Phys. Dark Univ.* 50 (2025) 102162. [arXiv:2508.14392](https://arxiv.org/abs/2508.14392), doi:10.1016/j.dark.2025.102162.

[25] G. Gu, X. Wang, Y. Wang, G.-B. Zhao, L. Pogosian, K. Koyama, J. A. Peacock, Z. Cai, J. L. Cervantes-Cota, M. Ishak, A. Shafieloo, R. Zhao, S. Ahlen, D. Bianchi, D. Brooks, T. Claybaugh, S. Cole, A. de la Macorra, A. de Mattia, P. Doel, S. Ferraro, J. E. Forero-Romero, E. Gaztañaga, S. Gontcho A Gontcho, G. Gutierrez, C. Hahn, C. Howlett, R. Kehoe, D. Kirkby, J.-P. Kneib, A. Kremin, O. Lahav, M. Landriau, L. Le Guillou, A. Leauthaud, M. Levi, M. Manera, A. Meisner, R. Miquel, J. Moustakas, A. Muñoz-Gutiérrez, S. Nadathur, J. A. Newman, N. Palanque-Delabrouille, W. Percival, F. Prada, I. Pérez-Ràfol, G. Rossi, L. Samushia, E. Sanchez, D. Schlegel, H.-J. Seo, D. Sprayberry, G. Tarlé, M. Walther, B. A. Weaver, P. Zarrouk, C. Zhao, R. Zhou, H. Zou, Author Correction: Dynamical dark energy in light of the DESI DR2 baryonic acoustic oscillations measurements, *Nature Astronomy* (Oct. 2025). doi:10.1038/s41550-025-02698-1.

[26] R.-J. Yang, X.-T. Gao, Observational constraints on purely kinetic k-essence dark energy models, *Chin. Phys. Lett.* 26 (2009) 089501. [doi:10.1088/0256-307X/26/8/089501](https://doi.org/10.1088/0256-307X/26/8/089501).

[27] C. L. Rodriguez, B. Farr, V. Raymond, W. M. Farr, T. B. Littenberg, D. Fazi, V. Kalogera, Basic Parameter Estimation of Binary Neutron Star Systems by the Advanced LIGO/Virgo Network, *Astrophys. J.* 784 (2014) 119. [arXiv:1309.3273](https://arxiv.org/abs/1309.3273), [doi:10.1088/0004-637X/784/2/119](https://doi.org/10.1088/0004-637X/784/2/119).

[28] J. Zuntz, M. Paterno, E. Jennings, D. Rudd, A. Manzotti, S. Dodelson, S. Bridle, S. Sehrish, J. Kowalkowski, CosmoSIS: modular cosmological parameter estimation, *Astron. Comput.* 12 (2015) 45–59. [arXiv:1409.3409](https://arxiv.org/abs/1409.3409), [doi:10.1016/j.ascom.2015.05.005](https://doi.org/10.1016/j.ascom.2015.05.005).

[29] M. Moresco, R. Jimenez, L. Verde, L. Pozzetti, A. Cimatti, A. Citro, Setting the Stage for Cosmic Chronometers. I. Assessing the Impact of Young Stellar Populations on Hubble Parameter Measurements, *Astrophys. J.* 868 (2) (2018) 84. [arXiv:1804.05864](https://arxiv.org/abs/1804.05864), [doi:10.3847/1538-4357/aae829](https://doi.org/10.3847/1538-4357/aae829).

[30] J. A. Lozano Torres, Generalized emergent dark energy in the late-time Universe, *Mon. Not. Roy. Astron. Soc.* 533 (2) (2024) 1865–1873. [doi:10.1093/mnras/stae1920](https://doi.org/10.1093/mnras/stae1920).

[31] B. Paxton, et al., Modules for Experiments in Stellar Astrophysics (MESA): Pulsating Variable Stars, Rotation, Convective Boundaries, and Energy Conservation, *Astrophys. J. Suppl.* 243 (1) (2019) 10. [arXiv:1903.01426](https://arxiv.org/abs/1903.01426), [doi:10.3847/1538-4365/ab2241](https://doi.org/10.3847/1538-4365/ab2241).

[32] S. Mandal, A. Singh, R. Chaubey, Cosmic evolution of holographic dark energy in $f(Q,T)$ gravity, *Int. J. Geom. Meth. Mod. Phys.* 20 (05) (2023) 2350084. [doi:10.1142/S0219887823500846](https://doi.org/10.1142/S0219887823500846).

[33] C. Larison, S. W. Jha, L. A. Kwok, Y. Camacho-Neves, Environmental Dependence of Type Ia Supernovae in Low-redshift Galaxy Clusters, *Astrophys. J.* 961 (2) (2024) 185. [arXiv:2306.01088](https://arxiv.org/abs/2306.01088), [doi:10.3847/1538-4357/ad0e0f](https://doi.org/10.3847/1538-4357/ad0e0f).

[34] C. Zhang, H. Zhang, S. Yuan, T.-J. Zhang, Y.-C. Sun, Four new observational $H(z)$ data from luminous red galaxies in the Sloan Digital Sky Survey data release seven, *Res. Astron. Astrophys.* 14 (10) (2014) 1221–1233. [arXiv:1207.4541](https://arxiv.org/abs/1207.4541), [doi:10.1088/1674-4527/14/10/002](https://doi.org/10.1088/1674-4527/14/10/002).

[35] D. Stern, R. Jimenez, L. Verde, M. Kamionkowski, S. A. Stanford, Cosmic Chronometers: Constraining the Equation of State of Dark Energy. I: $H(z)$ Measurements, *JCAP* 02 (2010) 008. [arXiv:0907.3149](https://arxiv.org/abs/0907.3149), [doi:10.1088/1475-7516/2010/02/008](https://doi.org/10.1088/1475-7516/2010/02/008).

[36] M. Moresco, et al., Improved constraints on the expansion rate of the Universe up to $z \sim 1.1$ from the spectroscopic evolution of cosmic chronometers, *JCAP* 08 (2012) 006. [arXiv:1201.3609](https://arxiv.org/abs/1201.3609), doi:10.1088/1475-7516/2012/08/006.

[37] M. Moresco, Raising the bar: new constraints on the Hubble parameter with cosmic chronometers at $z \sim 2$, *Mon. Not. Roy. Astron. Soc.* 450 (1) (2015) L16–L20. [arXiv:1503.01116](https://arxiv.org/abs/1503.01116), doi:10.1093/mnrasl/slv037.

[38] E. Gaztanaga, A. Cabre, L. Hui, Clustering of Luminous Red Galaxies IV: Baryon Acoustic Peak in the Line-of-Sight Direction and a Direct Measurement of $H(z)$, *Mon. Not. Roy. Astron. Soc.* 399 (2009) 1663–1680. [arXiv:0807.3551](https://arxiv.org/abs/0807.3551), doi:10.1111/j.1365-2966.2009.15405.x.

[39] C.-H. Chuang, Y. Wang, Modeling the Anisotropic Two-Point Galaxy Correlation Function on Small Scales and Improved Measurements of $H(z)$, $D_A(z)$, and $\beta(z)$ from the Sloan Digital Sky Survey DR7 Luminous Red Galaxies, *Mon. Not. Roy. Astron. Soc.* 435 (2013) 255–262. [arXiv:1209.0210](https://arxiv.org/abs/1209.0210), doi:10.1093/mnras/stt1290.

[40] C. Blake, et al., The WiggleZ Dark Energy Survey: Joint measurements of the expansion and growth history at $z < 1$, *Mon. Not. Roy. Astron. Soc.* 425 (2012) 405–414. [arXiv:1204.3674](https://arxiv.org/abs/1204.3674), doi:10.1111/j.1365-2966.2012.21473.x.

[41] N. G. Busca, et al., Baryon Acoustic Oscillations in the Ly- α forest of BOSS quasars, *Astron. Astrophys.* 552 (2013) A96. [arXiv:1211.2616](https://arxiv.org/abs/1211.2616), doi:10.1051/0004-6361/201220724.

[42] A. Oka, S. Saito, T. Nishimichi, A. Taruya, K. Yamamoto, Simultaneous constraints on the growth of structure and cosmic expansion from the multipole power spectra of the SDSS DR7 LRG sample, *Mon. Not. Roy. Astron. Soc.* 439 (2014) 2515–2530. [arXiv:1310.2820](https://arxiv.org/abs/1310.2820), doi:10.1093/mnras/stu111.

[43] N. Borghi, M. Moresco, A. Cimatti, Toward a Better Understanding of Cosmic Chronometers: A New Measurement of $H(z)$ at $z \sim 0.7$, *Astrophys. J. Lett.* 928 (1) (2022) L4. [arXiv:2110.04304](https://arxiv.org/abs/2110.04304), doi:10.3847/2041-8213/ac3fb2.

[44] G.-B. Zhao, et al., The clustering of the SDSS-IV extended Baryon Oscillation Spectroscopic Survey DR14 quasar sample: a tomographic measurement of cosmic structure growth and expansion rate based on optimal redshift weights, *Mon. Not. Roy. Astron. Soc.* 482 (3) (2019) 3497–3513. [arXiv:1801.03043](https://arxiv.org/abs/1801.03043), doi:10.1093/mnras/sty2845.

[45] S. Alam, et al., The clustering of galaxies in the completed SDSS-III Baryon Oscillation Spectroscopic Survey: cosmological analysis of the DR12 galaxy sample, *Mon. Not. Roy.*

Astron. Soc. 470 (3) (2017) 2617–2652. [arXiv:1607.03155](https://arxiv.org/abs/1607.03155), doi:10.1093/mnras/stx721.

[46] Y. Wang, et al., The clustering of galaxies in the completed SDSS-III Baryon Oscillation Spectroscopic Survey: tomographic BAO analysis of DR12 combined sample in configuration space, Mon. Not. Roy. Astron. Soc. 469 (3) (2017) 3762–3774. [arXiv:1607.03154](https://arxiv.org/abs/1607.03154), doi:10.1093/mnras/stx1090.

[47] L. Perivolaropoulos, F. Skara, Challenges for Λ CDM: An update, New Astron. Rev. 95 (2022) 101659. [arXiv:2105.05208](https://arxiv.org/abs/2105.05208), doi:10.1016/j.newar.2022.101659.

[48] R. Giostri, M. V. dos Santos, I. Waga, R. R. R. Reis, M. O. Calvão, B. L. Lago, From cosmic deceleration to acceleration: new constraints from SN Ia and BAO/CMB, JCAP 03 (2012) 027. [arXiv:1203.3213](https://arxiv.org/abs/1203.3213), doi:10.1088/1475-7516/2012/03/027.

[49] D. Brout, et al., The Pantheon+ Analysis: Cosmological Constraints, Astrophys. J. 938 (2) (2022) 110. [arXiv:2202.04077](https://arxiv.org/abs/2202.04077), doi:10.3847/1538-4357/ac8e04.

[50] N. Suzuki, et al., The Hubble Space Telescope Cluster Supernova Survey: V. Improving the Dark Energy Constraints Above $z > 1$ and Building an Early-Type-Hosted Supernova Sample, Astrophys. J. 746 (2012) 85. [arXiv:1105.3470](https://arxiv.org/abs/1105.3470), doi:10.1088/0004-637X/746/1/85.

[51] D. M. Scolnic, et al., The Complete Light-curve Sample of Spectroscopically Confirmed SNe Ia from Pan-STARRS1 and Cosmological Constraints from the Combined Pantheon Sample, Astrophys. J. 859 (2) (2018) 101. [arXiv:1710.00845](https://arxiv.org/abs/1710.00845), doi:10.3847/1538-4357/aab9bb.

[52] D. J. Eisenstein, et al., Detection of the Baryon Acoustic Peak in the Large-Scale Correlation Function of SDSS Luminous Red Galaxies, Astrophys. J. 633 (2005) 560–574. [arXiv:astro-ph/0501171](https://arxiv.org/abs/astro-ph/0501171), doi:10.1086/466512.

[53] N. Myrzakulov, M. Koussour, D. J. Gogoi, A new $\Omega_m(z)$ diagnostic of dark energy in general relativity theory, Eur. Phys. J. C 83 (7) (2023) 594. [arXiv:2303.04640](https://arxiv.org/abs/2303.04640), doi:10.1140/epjc/s10052-023-11794-3.

[54] J. S. Alcaniz, J. P. Neto, F. S. Queiroz, D. R. da Silva, R. Silva, The Hubble constant troubled by dark matter in non-standard cosmologies, Sci. Rep. 12 (1) (2022) 20113, [Erratum: Sci. Rep. 13, 209 (2023)]. [arXiv:2211.14345](https://arxiv.org/abs/2211.14345), doi:10.1038/s41598-022-24608-5.

[55] M. Abdul Karim, et al., DESI DR2 Results II: Measurements of Baryon Acoustic Oscillations and Cosmological Constraints, arXiv preprint (3 2025). [arXiv:2503.14738](https://arxiv.org/abs/2503.14738).